

2

3

4

Hydrologic Controls on Aperiodic Spatial Organization of the Ridge Slough Patterned Landscape

5

6

7

8

9

10

Stephen T. Casey¹, Matthew J. Cohen^{1,*}, Subodh Acharya¹, David A. Kaplan²
and James W. Jawitz³

11

12

13

14

15

16

17

1 – School of Forest Resources and Conservation, University of Florida, Gainesville FL

18

2 – Engineering School of Sustainable Infrastructure and Environment, Environmental Engineering Sciences Department,

19

University of Florida, Gainesville FL

20

3 – Soil and Water Science Department, University of Florida, Gainesville, FL

21

22

* - Corresponding Author (email: mjc@ufl.edu; phone 352.846.3490)

23

24 **Abstract**

25 A century of hydrologic modification has altered the physical and biological drivers of landscape processes in the
26 Everglades (Florida, USA). Restoring the ridge-slough patterned landscape, a dominant feature of the historical system, is
27 a priority, but requires an understanding of pattern genesis and degradation mechanisms. Physical experiments to evaluate
28 alternative pattern formation mechanisms are limited by the long time scales of peat accumulation and loss, necessitating
29 model-based comparisons, where support for a particular mechanism is based on model replication of extant patterning
30 and trajectories of degradation. However, multiple mechanisms yield a central feature of ridge-slough patterning (patch
31 elongation in the direction of historical flow), limiting the utility of that characteristic for discriminating among
32 alternatives. Using data from vegetation maps, we investigated the statistical features of ridge-slough spatial patterning
33 (ridge density, patch perimeter, elongation, patch-size distributions, and spatial periodicity) to establish more rigorous
34 criteria for evaluating model performance, and to inform controls on pattern variation across the contemporary system.
35 Mean water depth explained significant variation in ridge density, total perimeter, and length:width ratios, illustrating
36 important pattern response to existing hydrologic gradients. Two independent analyses (2-D periodograms and patch size
37 distributions) provide strong evidence against regular patterning, with the landscape exhibiting neither a characteristic
38 wavelength nor a characteristic patch size, both of which are expected under conditions that produce regular patterns.
39 Rather, landscape properties suggest robust scale-free patterning, indicating genesis from the coupled effects of local
40 facilitation and a global negative feedback operating uniformly at the landscape-scale. Critically, this challenges
41 widespread invocation of scale-dependent negative feedbacks for explaining ridge-slough pattern origins. These results
42 help discern among genesis mechanisms and provide an improved statistical description of the landscape that can be used
43 to compare among model outputs, as well as to assess the success of future restoration projects.

44

45 *Keywords:* regular patterning, scale-free patterning, robust criticality, scaling relationships, ridge slough landscape,
46 periodogram analysis, Everglades, wetland restoration.

47 **1 Introduction**

48 The coupling of ecosystem processes operating at different scales can cause vegetation communities to form a
49 wide variety of spatial patterns (Borgogno et al., 2009), ranging from highly regular striping, stippling or maze-like
50 patterns in woodland landscapes (Ludwig et al., 1999), tidal mud flats (Weerman et al., 2012), and boreal peatlands
51 (Eppinga et al., 2010) to scale-free patterning in semi-arid landscapes (Kefi et al., 2007; Scanlon et al., 2007). The
52 mechanisms that produce these patterns are integral to understanding landscape origins, and thus for predicting
53 appropriate remedies where patterns and underlying processes have been degraded and require restoration. The spatial
54 arrangement of vegetation on the landscape has long been viewed as a manifestation of the dominant interactions and
55 drivers (Hutchinson, 1957; Levin, 1992), and the scales at which they operate. By quantifying this spatial arrangement we
56 can make process-based inferences about the underlying mechanisms (Gardner et al., 1987; Turner, 2005).

57 The ridge-slough landscape comprised ~55 % of the pre-development Everglades in southern Florida (McVoy et
58 al., 2011). However, processes that created, and in some places still maintain, the characteristic ridge-slough patterning
59 are only partially understood (Science Coordination Team, 2003; Larsen et al., 2011; Cohen et al., 2011). The landscape
60 pattern consists of flow-parallel bands of higher-elevation ridges dominated by emergent sedge sawgrass (*Cladium*
61 *jamaicense*), interspersed within a matrix of lower-elevation sloughs (ca. 25 cm lower in the best conserved portions of
62 the landscape; Watts et al., 2010), which contain a variety of submerged and emergent herbaceous macrophytes. The
63 Everglades has undergone massive hydrologic modification through the construction of a system of levees and canals
64 over the past century (Light and Dineen, 1994), and ensuing ecological degradation has prompted a complex, expensive,
65 and ambitious restoration effort. Because the ridge-slough landscape was so prevalent in the pre-development system,
66 pattern restoration is a central priority (SCT 2003; McVoy et al., 2011). The mechanisms that control the emergence of
67 patterning and explain variation in pattern geometry are thus integral to specifying hydrologic restoration objectives.

68 To understand the landscape processes that produce patterning, and by extension gain insight into how to restore
69 them (Pickett and Cadenasso, 1995), requires a testable mechanistic framework for pattern genesis and maintenance.
70 However, experiments to test alternative mechanisms are constrained by the spatial extent and time scales of peat
71 accumulation responses. Paradoxically, compartmentalization by the extensive canal and levee system has created
72 artificial gradients that are informative for assessing trajectories of landscape pattern degradation. Here we focus on

73 Water Conservation Area 3 (WCA-3), located in the central Everglades, an area historically dominated by the ridge-
74 slough landscape (Fig. 1), and where the best conserved patterning is found. The hydrologic gradient in WCA-3 spans
75 from relatively dry (i.e., short hydroperiod) conditions in the north due to major canals that drain water to the southeast, to
76 extended inundation (i.e., long hydroperiod) in the south and southeast due to impoundment caused by US41/Tamiami
77 Trail (which runs orthogonal to flow) and the L-67 levee. The best conserved patterning (SCT, 2003; Watts et al. 2010) is
78 found between these hydrologic extremes.

79 Several alternative hypotheses have been proposed to explain ridge slough patterns, and all have been evaluated
80 using process-based models. The mechanisms invoked vary and include evaporative nutrient redistribution (Ross et al.,
81 2006; Cheng et al., 2011), flow-driven sediment redistribution from sloughs to ridges (Larsen et al., 2007; Larsen and
82 Harvey 2011; Lago et al., 2010), self-optimization of patterning for discharge and hydroperiod (Cohen et al., 2011;
83 Kaplan et al., 2012; Heffernan et al., 2013), and a suite of mechanisms that couple pattern-hydroperiod effects with
84 directional local facilitation processes (i.e., where patches expand more rapidly in one direction than another; Acharya et
85 al., 2015). Clearly, these mechanisms are not mutually exclusive, so process models have sought to explore the
86 sufficiency of each alternative, while acknowledging the potential that multiple processes may overlap. One central
87 criterion used to evaluate the models has been whether simulations can produce morphologies qualitatively consistent
88 with the extant landscape (principally replicating the elongation of patches in the flow direction). To date, however,
89 almost all models either accomplish (Ross et al., 2006; Larsen and Harvey, 2010; Lago et al., 2010; Cheng et al., 2011;
90 Acharya et al., 2015) or strongly imply (Heffernan et al., 2013) patch elongation (albeit sometimes under conditions
91 markedly different than those observed in the Everglades), limiting discrimination among pattern genesis mechanisms
92 and highlighting the need for a more rigorous and quantitative characterization of landscape pattern.

93 To better characterize patterns in both the best conserved state and spanning a gradient of degradation requires
94 spatial analyses that yield quantitative properties against which model outputs can be compared. Although numerous
95 metrics have been developed to quantify different pattern attributes (Wu et al., 2007; Yuan et al., 2015), significant gaps
96 in our understanding of how to interpret these metrics remain (Turner, 2001; Rummel and Csillag, 2003). Real landscapes
97 clearly depart from regular Euclidean geometry, making characterization problematic in some cases (Mandelbrot, 1983).
98 Likewise, changes in mapping procedures (e.g., grain size, extent, classification schemes) can yield significantly different

99 metric values for the same landscape (Li and Wu, 2004). To remedy some of these issues, we focused on a set of
100 relatively direct and easily interpreted metrics of fundamental aspects of the pattern, and used multiple maps produced
101 with varying methods to rule out mapping-related artifacts. We were interested in three aspects of landscape patterning:
102 density and shape statistics, patch-size distributions, and spectral (i.e., pattern wavelength) characteristics. For each
103 aspect, we explored the magnitude of site-to-site variation and the support for hydrologic control of that variation.

104 Density and shape statistics focus on the most basic and intuitive geometric properties of the landscape: areal
105 coverage of the patch types (density), landscape pattern complexity (perimeter), and the degree of elongation. While
106 inundation has been shown to control species composition (Givnish et al., 2008; Zweig and Kitchens, 2008; Todd et al.,
107 2010), the relationship between hydrologic drivers and other aspects of landscape pattern remain relatively unknown, so
108 this effort also serves as an inventory of hydrologic controls on pattern geometry.

109 Patch size distributions (i.e., frequency of different patch sizes) have been used in many systems to identify
110 underlying landscape processes (e.g., Manor and Shnerb, 2008a; Kefi et al., 2011; Bowker and Maestre, 2012; Weerman
111 et al., 2012). For example, regular patterning is associated with a characteristic patch size (Rietkerk and van de Koppel,
112 2008; von Hardenberg, 2010), arising in response to an inhibitory feedback operating at a particular spatial scale (van de
113 Koppel and Crain, 2002) that limits patch expansion. Under these conditions, there should be a distinct mode in patch
114 area distribution, or at least the absence of very large patches (Manor and Shnerb, 2008; von Hardenberg, 2010; Kefi et
115 al., 2014). In contrast, patch size distributions that follow a power-law (i.e., $y=x^\alpha$, where α is a scaling parameter) lack a
116 characteristic spatial scale (e.g., Scanlon et al., 2007) and may suggest genesis mechanisms that operate equally across
117 scales. Correspondingly, power law distributions are often referred to as scale-free, in that the distribution form remains
118 the same regardless of the measurement scale.

119 Scale-free distributions can arise via a number of mechanisms (Newman et al., 2005). In a landscape where grid
120 cells are randomly occupied, patch distributions show relatively few large patches, up to a critical density (~ 0.59 ; known
121 as the percolation threshold) at which patches span the domain, yielding power-law area scaling. At densities slightly
122 above and below the percolation threshold, area distributions depart from power-laws. The narrow range of density space
123 over which scale-free area distributions emerge would seem to suggest that this mechanism is rare. However, some

124 systems can endogenously maintain themselves near this critical point in a phenomenon referred to as self-organized
125 criticality (Bak et al., 1989). This is accomplished through disturbance processes that propagate via patch contiguity (e.g.,
126 forest fires, see Drossel and Schwabl, 1992), maintaining patterns near the percolation threshold through a cycle of large-
127 scale disturbance and slow recovery (Pascual and Guichard, 2005).

128 Alternatively, power-law scaling of patch areas can arise from the coupled action of local facilitation, which
129 causes patches to expand, and competition for a global resource (Pascual et al., 2002; Scanlon et al., 2007) that ultimately
130 limits the density of that patch type at the landscape scale. In contrast to regular patterning mechanisms, these feedback
131 processes limit landscape-level patch density, but not the size of individual patches, leading to the creation, via local
132 facilitation, of very large patches. This is known as robust criticality because power-law scaling in response can occur
133 over a wide range of external conditions and patch densities, including densities well below the percolation threshold.
134 Robust criticality has been noted in Everglades vegetation distributions (Foti et al., 2012), as well as in a variety of
135 dryland vegetation patterns (Kefi et al., 2011). Widespread occurrence of both local facilitation and global resource
136 competition in ecological systems suggests this process may operate in a multitude of landscapes.

137 Finally, spectral characteristics provide insights on the presence and wavelength of regular landscape pattern.
138 Useful information about the scale at which spatial feedbacks operate in self-organized systems has been obtained by
139 evaluating 2-dimensional pattern periodicity (Couteron, 2002; Kefi et al., 2014). This is particularly important in the
140 Everglades because the prevailing conceptual model for ridge-slough pattern genesis invokes interactions between spatial
141 feedbacks operating on different characteristic scales, resulting in a pattern wavelength of approximately 150 m in the
142 direction perpendicular to historical flow (SCT, 2003; Watts et al., 2010). Several models (e.g. Ross et al., 2006; Lago et
143 al., 2010; Cheng et al., 2011) produce distinctly periodic landscapes, which arise from the action of local facilitation
144 feedbacks and, crucially, negative feedbacks on patch expansion that operate at a characteristic scale. In contrast, the
145 feedback between hydroperiod and landscape geometry suggested by Cohen et al. (2011), enumerated by Heffernan et al.
146 (2013), and tested at the landscape scale in Kaplan et al. (2012), operates at the global-scale, implying no characteristic
147 spatial scale. To that end, we tested the hypothesis that the ridge-slough landscape is regularly patterned (i.e., exhibits a
148 characteristic wavelength), consistent with scale-specific negative feedbacks, or whether the landscape lacks periodicity,
149 consistent with scale-free feedbacks.

150 Together, these spatial analyses encompass a novel and rigorous set of metrics for improved quantification of
151 observed and modeled landscape pattern. While developed to improve descriptions of the ridge-slough pattern, these
152 metrics may also be useful for identifying pattern and discriminating genesis mechanisms in other patterned landscapes.

153

154 **2 Methods**

155 **2.1 Vegetation and hydrologic data**

156 We used multiple vegetation maps of the central Everglades, which vary in scale, extent, mapping schemes, and
157 time frame. For all maps, we aggregated vegetation types into binary classes (reclassification scheme in Table S2) of
158 ridges (*value* = 1) and sloughs (*value* = 0). Our primary map (M1) was produced by the South Florida Water Management
159 District (SFWMD) using 1:24 000-scale color infrared photos from September 1994 (Rutchev, 2005). This map was
160 chosen due to its large, continuous spatial extent and fine mapping detail. The presence of small (<25 m²) landscape
161 features permitted us to select raster representation of dominant vegetation at high (i.e., 1 x 1 m cells) resolution. While
162 the presence of small features does not imply map accuracy at that fine scale, it does imply loss of patch geometric detail
163 with larger cells. Features at this scale can be subject to mapping error and artifacts, likely under-representing their
164 prevalence. As such, patches below 100 m² were omitted from patch-level analyses.

165 We selected 33 6×6 km sites to span the range of current hydrological conditions (i.e., dry in northern areas to wet
166 in southern areas; Fig. 1). We sought to maximize the number of sites with minimal overlap, while avoiding roads and
167 canals. All sites except 20–22 and 32–33 were rotated to align with the prevailing direction of patch elongation (15°
168 counterclockwise). Ridge cells were grouped into patches if they shared at least one edge with an adjacent ridge (i.e.,
169 a von Neumann neighborhood).

170 Within each site, *point-specific* daily average water depths at a grid spacing of 200 m were obtained from the
171 Everglades Depth Estimation Network (EDEN) xyLocator (<http://sofia.usgs.gov/eden/edenapps/xylocator.php>). We note
172 these water depths are spatially interpolated from a network of water elevation monitoring stations and, as such, represent
173 only an estimate of actual conditions. *Site-specific* mean water depth (MWD) values were obtained by averaging all point-
174 specific values in each site over the period of record from 1991–2010.

175 We used two additional maps (M2 and M3), which vary in spatial extent, resolution, and sampling date, to
176 corroborate M1 analyses and test map resolution effects and temporal changes. M2 was generated from 1:24 000 scale
177 aerial photographs taken in 2004 (RECOVER 2014) and rasterized at 50 m resolution. M3 was generated from 1 m
178 resolution digital orthophotos and rasterized at 1 m (Nungesser, 2011). Methodological details for both M2 and M3 are
179 given as supplementary information.

180 **2.2 Shape and density**

181 We compared ridge density, edge density, and elongation across sites. Ridge density is the proportion of ridge area
182 to site area, while edge density is total patch perimeter divided by site area. In order to measure elongation, E , we first
183 identify individual lengths and widths (l and w , respectively) as any group of contiguous ridge cells (i.e. unbroken by
184 slough cells) along a row or column. Elongation is the ratio of the mean of these contiguous row and column sections:

$$185 \quad E = \frac{\frac{1}{n_c} \sum l}{\frac{1}{n_r} \sum w} = \frac{n_r}{n_c} \quad (1)$$

186 where n_r and n_c represent the number of contiguous rows and columns. Elongation simplifies to their ratio since the
187 summation terms both yield the total number of ridge cells. Elongation metrics are sensitive to orientation differences
188 between the grid and landscape features. Sites with tortuous flow paths or a poorly aligned grid will underestimate E . We
189 provide estimates of grid alignment with feature orientation as a mean patch angle, \bar{A}_p , where A_p is the angle between the
190 grid y axis and the major axis of an ellipse with the same second moment as the patch.

191 Hydrologic trends were identified by regressing MWD against site-level metrics, and were considered statistically
192 significant at $p < 0.05$. For analyses that are highly dependent on mapping resolution (i.e., edge density), we omit M1 sites
193 north of Interstate-75, as these were mapped using significantly lower resolution than those to the south (Rutchev, 2005).
194 Because elongation values are dominated by the domain shape at very high ridge densities, we omitted sites where ridge
195 density exceeded 0.8.

196 **2.3 Patch size distributions**

197 Patch size scaling properties were evaluated by comparing empirical distributions to several candidate models.
198 Patch size distributions can be described in terms of their complementary cumulative distribution function (CCDF), which

199 gives the probability that the area of an observed patch is greater than or equal to a given area, x . Preliminary analyses
 200 showed that empirical CCDFs exhibited extremely heavy tails consistent with power laws, but only above a minimum
 201 cutoff, below which patches were less abundant and the CCDFs were rounded. This form is in relative agreement with
 202 both the Generalized Pareto (GP) and truncated lognormal distributions. The GP is given by its CCDF as

$$203 \quad P(x) = \begin{cases} \left(1 + \frac{k(x-x_{min})}{\delta}\right)^{-\frac{1}{k}} & \text{for } k \neq 0 \\ \exp\left(-\frac{x-x_{min}}{\delta}\right) & \text{for } k = 0 \end{cases} \quad (2)$$

204 for $x \geq x_{min}$ when $k \geq 0$, and for $x_{min} \leq x \leq (x_{min} - \delta/k)$ when $k < 0$. The GP reduces to the exponential distribution when $k =$
 205 0 and $x_{min} = 0$, and reduces to a power-function when $k > 0$ and $x_{min} = \delta/k$. For $k > 0$ and $x_{min} < \delta/k$ the GP shows
 206 exponential-like behavior for low values of x , while the tail asymptotically approaches a power law for $x \gg x_{min}$. Within
 207 this range of parameters, δ indicates the curvature in the upper end of the distribution (higher values correspond to greater
 208 curvature and hence, relatively fewer small patches), while k indicates the scaling properties of the tail, such that for $x \gg$
 209 x_{min} , the power-law scaling exponent α approaches $\alpha^* = (1 + 1/k)$ (Pisarenko and Sornette, 2003). Where the GP fits the
 210 data well, we can use the estimated parameters as general information about patch size scaling properties. The CCDF for
 211 a truncated lognormal distribution uses the mean ($\mu_{\ln x}$) and standard deviation ($\sigma_{\ln x}$) of $\ln(x)$.

$$212 \quad P(x) = \frac{\operatorname{erf}\left(\frac{\sqrt{2}[\mu_{\ln x} - \ln(x)]}{2\sigma_{\ln x}}\right) + 1}{\operatorname{erf}\left(\frac{\sqrt{2}[\mu_{\ln x} - \ln(x_{min})]}{2\sigma_{\ln x}}\right) + 1} \quad x \geq x_{min} \quad (3)$$

213
 214
 215

We compared empirical distributions to synthetic data sets from Monte Carlo simulations ($n = 20,000$ per model)

216 and compared candidate distributions based on log-likelihood ratios and significance values (Clauset et al., 2009).

217 Distribution testing details are given in SI.

218 **2.4 Spectral characteristics**

219 Spectral characteristics of the ridge-slough landscape were evaluated from 2-D periodograms generated following
 220 the methods of Mugglestone and Renshaw (1998). In brief, we constructed a discrete 2-D Fourier transform (available in
 221 most computational software packages) for each binary vegetation map (Kefi et al., 2014), and then took the absolute
 222 value to obtain the real number component. The resulting 2-D periodogram (i.e. spectral density) is a grid representing the

223 magnitude of cosine and sine waves of possible wavenumbers (i.e. spatial frequencies), and orientations to the spectrum.
224 Values were averaged across all orientations in equally spaced wavenumber bins to generate radial spectra (*r* spectra),
225 which indicate the relative spectral density for each corresponding wavenumber bin. Local maxima indicate dominant
226 wavelengths, and thus suggest the presence of spatial periodicity (Couteron, 2002; Kefi et al., 2014), or regular
227 patterning. The absence of local maxima indicates an aperiodic landscape. Because the ridge-slough pattern has been
228 described as regular in the direction orthogonal to flow, we generated both lateral and longitudinal *r* spectra derived from
229 the spectral densities observed within $\pm 10^\circ$ perpendicular and parallel to the main axis of pattern elongation. For both
230 directions, we noted the wavelength at which either clear spectral peaks (i.e., for periodic patterns) or locations of spectral
231 shouldering (i.e. slope breaks), which may indicate a secondary scale-dependent feedback mechanism, were evident.
232 Since smaller features are underrepresented in low resolution maps, we omitted wavelengths $< 10\text{m}$ from our analyses.

233

234 **3 Results**

235 **3.1 Visual comparisons**

236 Visual inspection of the vegetation maps reveals a remarkable range of pattern morphology (Fig. 1). Ridges in
237 northwestern sites (1–5) show pronounced striping, which is less apparent in southern sites (18–22), where ridges appear
238 more elliptical. Eastern sites located below I-75 (5, 9, 13, 14, 17, 28–33) show fine-scale speckling and disaggregation,
239 with sites 14, 28 and 29 appearing random, with faint outlines of historic pattern.

240 Individual ridges exhibit numerous connections between adjacent elongated portions, with larger patches forming
241 complex webs composed of multiple individual elements. Although this behavior is apparent in all sites, it appears to be
242 density dependent, with most of the landscape spanned by one large patch in denser sites (e.g., 2, 5, 8, 9, 11–13, 23–28,
243 30–33). Within sites, large patches are always more web-like than smaller ones, which appear more distinctly separated.

244 **3.2 Density and shape**

245 Ridge density was negatively correlated to MWD (Fig. 2a; $R^2 = 0.38$, $p = 0.0002$). Deviation from this association
246 was similar across maps and related to geographic position. Specifically, ridge densities in the eastern half of the domain
247 (sites 9, 13, 14, 17, 23–33) were consistently higher than in the west, suggesting a strong east–west control on density.
248 The correlation between MWD and ridge density increased markedly when sites were partitioned into east and west

249 blocks (east: $R^2 = 0.81$, $p < 0.0001$; west: $R^2 = 0.61$, $p = 0.0004$). Based on recent aerial imagery, low ridge density in site
250 1 is a misclassification of sparse sawgrass prairies as slough; that site was omitted from regression analyses.

251 Site-level elongation was also strongly correlated to MWD (Fig. 2b; $R^2 = 0.65$, $p < 0.0001$). Sites with ridge
252 densities greater than 0.8 showed elongation values much lower than this trend. Average patch orientations (\bar{A}_p) indicate
253 consistency between the grid and feature elongation (i.e., \bar{A}_p values close to zero; Table S1). Sites with values of $|\bar{A}_p| \geq 5^\circ$
254 (e.g., 1, 22), may be underestimated due to mismatch between patch orientation and map orientation. Finally, edge density
255 was strongly correlated to MWD, indicating greater perimeter at deeper sites (Fig. 2c; $R^2 = 0.79$, $p < 0.0001$).

256 3.3 Patch size distributions

257 Patch area distributions were consistent with the Generalized Pareto distribution (Fig. 3c), with 16 of 25 sites
258 passing GP Monte Carlo tests for M1 and 4 of 9 passing for M3 (Table S1). The majority of sites that were not significant
259 contained extremely large patches, but had little deviation in the rest of the distribution; in some cases (e.g., sites 2, 5, 8,
260 9, 11, 12, 13, 28, 31) the largest patch was over an order of magnitude larger than predicted based on the GP distribution.
261 All these sites with extremely large patches have ridge densities above or very close to the percolation threshold of a
262 square lattice (~ 0.59 , Stauffer, 1995). Above this percolation threshold, the largest patch becomes “over-connected”,
263 suggesting that failure of Monte Carlo tests within this group may be density driven, rather than a result of an underlying
264 patterning mechanism. Note that these sites are largely located in the north and eastern sections of the study area, a region
265 typified by high ridge densities. The presence of tree islands, a third landform modality distinct from ridges and sloughs,
266 may also affect patch scaling relationships; however, we neglect these effects here because across all blocks tree islands
267 represent less than 10% of the area, and often much less. The log-normal distribution was significant in only 4 of 25 sites
268 for M1 and 2 of 9 sites for M3. Although these sites (15, 16, 19, 21) showed slight rounding in the extreme tail, log-
269 likelihood ratios were not different enough to distinguish between the two candidate distributions (Table S1).

270 Within each map, GP parameters were remarkably consistent across sites, with almost constant estimates of k and
271 δ for sites that passed Monte Carlo tests (Table S1). Area scaling in the tail of the distribution is illustrated by α^*
272 (analogous to the scaling exponent of a power-law distribution) = 1.77 ± 0.06 for M1 and 1.87 ± 0.13 for M3. The δ
273 parameter indicates how sharply the distribution head deviates from a power-law, with larger values indicating that

274 smaller patch areas are exceedingly rare. For M1 and M3, $\delta = 474 \pm 88$ and 1490 ± 219 ; these differences are likely due to
275 map resolution, with M3 under-representing smaller patches.

276 **3.4 Spectral characteristics**

277 We found no evidence of periodicity in either the lateral or longitudinal r spectra. The absence of peak values other
278 than the smallest wavenumber indicates that no dominant pattern wavelength exists, a finding consistent across
279 hydrologic conditions and pattern morphologies (Fig. 3a, Supplement Fig. S7). Spearman correlations, ρ , show the r
280 spectra is nearly perfectly approximated by a monotonic function across all sites (Table S1), with $\rho < -0.99$ for both
281 lateral and longitudinal r spectra. As with patch-scaling relationships, tree islands may introduce some noise in the
282 observed r spectra, however this effect is likely to be small, given that they constitute less than 10% of the landscape.

283 For both lateral and longitudinal directions, the form of the r spectra appeared to contain a mix of both power law
284 and exponential scaling. Lateral r spectra largely appear linear in log-log space (i.e. power law form) at higher
285 wavenumbers, while rounding towards an exponential (i.e. curved) at lower wavenumbers. This curvature appears over a
286 wider range of wavenumbers for longitudinal spectra, but the morphology and mean transition location are same laterally
287 and longitudinally. Sites with the best conserved patterning (e.g. sites 2, 5, 11, 20) show more localized curvature in
288 lateral r spectra compared to degraded sites, potentially signifying the action of a secondary, scale-dependent patterning
289 mechanism. We note, however, that this finding is inconsistent with proposed patterning mechanisms that invoke a
290 characteristic wavelength in the lateral direction but include no mechanism to generate regular patterning in the
291 longitudinal direction. Alternatively, this shouldering may result from undersampling large features at low wavenumbers
292 due to a limited domain size.

293

294 **4 Discussion**

295 **4.1 Water depth controls pattern attributes**

296 Our results provide strong observational support for water depth as a dominant control on several key shape and
297 density properties of the ridge-slough landscape. Although these findings are correlative and not necessarily mechanistic,
298 they align with current understanding about the mechanisms that create, maintain, and degrade the landscape. The
299 observed decline in ridge abundance with MWD is consistent with conceptual models that predict that changes in water

300 levels precipitate transitions between ridge and slough by modifying production and respiration dynamics (Givnish et al.,
301 2008; Watts et al., 2010) and inducing state changes in vegetation composition (Zweig et al., 2008). The implication that
302 these dynamics differ in eastern and western sections of the study area was unexpected, and points to unexplained
303 controls on ridge expansion. The largest difference between the east and west trends occurs at low water depths,
304 indicating that this control is most pronounced in drier sites. In short, the deviation seen in eastern sites represents a
305 shifting of the relationship to favor sawgrass expansion in extremely dry sites, rather than a general reduction of the
306 hydrologic limitation (since deep sites remain the least affected).

307 Mean water depth also exerted strong control on ridge-slough pattern shape. The most salient features of the
308 pattern, elongation and perimeter, both showed strong dependence on MWD, with maximum elongation observed at low
309 to intermediate water depths and minimum edge density values at low water depths. This is consistent with ridge features
310 fragmenting into smaller, less elongated patches under deeper water conditions, a finding previously observed anecdotally
311 (McVoy et al., 2011) and in the spatial statistics of soil elevation (Watts et al., 2010). Likewise, sites with very low MWD
312 show a significant loss of pattern, with ridge densities approaching unity and elongation values that are largely isotropic.
313 The coherent response of these pattern features to hydrologic modification suggests promise for their use as restoration
314 performance measures (Yuan et al., 2015).

315 In this work we provide support for hydrological controls on ridge-slough pattern shape; however landscape
316 patterning (specifically ridge density and elongation) has also been shown to exert reciprocal control on regional
317 hydrology (Kaplan et al., 2012). Loss of sloughs in sites with very low MWD alters drainage characteristics. Coupled to
318 observations of patch fragmentation in sites with higher water depths, these results strongly reinforce the commanding
319 role of hydrology in maintaining landscape pattern, indicating that reversal of modern hydrologic modification is
320 paramount for ongoing restoration.

321

322 **4.2 The ridge-slough landscape is aperiodic and scale-free**

323 Both spatial periodogram results and patch size distributions strongly suggest the ridge-slough landscape pattern is
324 aperiodic, a marked departure from extensive literature qualitatively describing the pattern as periodic (SCT 2003; Wetzel
325 et al., 2005; Ross et al., 2006; Larsen, 2007; Givnish et al., 2008; Larsen and Harvey, 2010; Lago et al., 2010; Watts et

326 al., 2010; Cheng et al., 2011; Nungesser, 2011; Sullivan et al., 2014). Because negative feedbacks operating at a
327 characteristic spatial scale result in regular patterning (Rietkerk and Van de Koppel, 2008), aperiodic patterning in the
328 ridge-slough landscape implies the absence, or least secondary importance, of such feedbacks, ruling out as the dominant
329 control on patterning many of the mechanisms invoked to explain pattern formation (Borgogno et al., 2009).

330 While our results clearly support the primacy of aperiodic patterning mechanisms, the r spectra in both lateral and
331 longitudinal directions do exhibit persistent curvature, whose location and degree appears dependant on both orientation
332 and pattern condition. This suggests ridge-slough patterning is secondarily influenced by scale-dependent (but
333 omnidirectional) feedbacks, possibly suggesting links with vegetative propagation or fire behavior. Additional
334 investigation and modeling, requiring higher resolution mapping, would be necessary to better understand the mode and
335 scale of these secondary feedbacks.

336 The observation that patch size distributions uniformly follow power-law scaling suggests a scale-free patterning
337 process. While power-law scaling can be produced via several mechanisms (Newman et al., 2005), our results can be used
338 to rule out some alternatives. For example, power-law scaling of patch areas can arise in systems near the percolation
339 threshold (i.e., at criticality), which occurs within a relatively narrow region of patch density. Observed patch area scaling
340 in our study occurs across a wide range of patch densities, suggesting robust criticality that comports with Foti et al.
341 (2012), who observed similar power-law scaling behavior over a wide range of vegetation types and densities.

342 Caution is warranted when using contemporary aerial imagery to infer pre-drainage landscape conditions; the first
343 aeriels were taken ~65 years after Everglades drainage began. Several pattern attributes (e.g., density, perimeter) may
344 adjust readily with hydrologic modification, and while some areas remain largely unchanged since initial imagery was
345 obtained, pattern in many other areas has degraded, sometimes entirely (Wu et al. 2006, Nungesser 2011). However,
346 pattern properties that are relatively invariant with hydrologic modification (e.g. the general forms of the r -spectrum and
347 patch area distributions) are more likely to reflect pre-drainage conditions. In contrast, while measures that vary with
348 hydrologic modification are correlative, they remain useful for understanding landscape responses to hydrologic forcing,
349 but may be less informative for inferring pre-drainage conditions and long-term processes such as landscape formation.

350 Self-organized criticality can also produce power-law scaling at varying densities (i.e., far from the percolation
351 threshold), but requires large temporal variation in ridge density as the system endogenously readjusts towards criticality

352 following disturbances (Pascual and Guichard, 2005). Recent paleoecological evidence (Bernhardt and Willard, 2010)
353 suggests that ridge-slough configurations and densities have remained relatively stable since initial formation 2700 years
354 before present, though temporal variation in density (e.g., during the Medieval Warm Period) may have been sufficient to
355 modestly alter landscape pattern metrics. Moreover, no documented disturbance regime exhibits the characteristic
356 separation of time scales between growth and disturbance associated with self-organized criticality. While peat fires could
357 be invoked, there is little evidence for widespread incidence and large-scale impacts of these prior to modern hydrologic
358 modification (McVoy et al., 2011).

359 Rather, power-law scaling in patch areas over a range of densities along environmental gradients is consistent with
360 robust criticality, wherein local facilitation induces clustering (i.e., patch growth) while a global limitation maintains
361 landscape heterogeneity (Pascual and Guichard, 2005). Although robust criticality is typically suggested in isotropic
362 landscapes, Acharya et al. (2015) recently showed that anisotropy in the local facilitation kernel of a robust criticality
363 model can produce directional banding without periodicity, yielding simulated ridge-slough patterns with high statistical
364 and visual fidelity to the observed landscape. Local facilitation may take the form of autogenic peat accretion (Larsen et
365 al., 2007), clonal propagation of sawgrass (Brewer, 1996), nutrient accumulation dynamics (Cohen et al., 2009, Larsen et
366 al. 2015), or local seed dispersal, although the relative importance and directionality of these mechanisms remains
367 unknown (Acharya et al., 2015). Screening possible mechanisms for anisotropic local facilitation emerges from our
368 analysis as a priority for future investigations.

369 Several candidate processes could limit patch expansion in the ridge slough landscape. Each implies a distinct
370 spatial pattern geometry, and we can use the extant scale-free and aperiodic geometry to evaluate their respective
371 plausibilities. A key distinction between limiting processes that produce periodic versus scale-free patterning is the spatial
372 range over which the limiting factor acts (Manor and Shnerb, 2008a; von Hardenberg, 2010). When the limiting effect of
373 patch expansion locally is spread uniformly across the landscape, the effect is considered global or uniform. Conversely,
374 when the limiting effect act in a more localized manner, limitation gradients can develop and produce periodic patterning.

375 Phosphorus limitation and sediment transport mechanisms are both potentially important feedbacks on patch
376 expansion. While phosphorus is strongly limiting of primary production in the Everglades (Noe et al., 2001), and can be
377 dramatically enriched in tree-islands (Wetzel et al. 2009) and ridges (Ross et al. 2006) via multiple mechanisms, this

378 process of local enrichment and depletion is inconsistent with robust criticality. Indeed, the presence of strong local
379 phosphorus gradients indicates that limitation feedbacks are distinctly local, and not spread uniformly across the
380 landscape. If phosphorus limitation were the dominant control, the result would be regular patterning. Similarly, sediment
381 transport mechanisms (Larsen et al., 2007; Lago et al., 2010) yield a balance between entrainment and deposition
382 governed by focused flow in sloughs, the velocity of which is controlled by cross-sectional occlusion of flow by ridges.
383 Because patch geometry is controlled by local heterogeneity in flow velocity, this suggests an inhibitory feedback
384 operating at a limited spatial scale, as the velocity field responds most strongly to local flow occlusion.

385 Water level (and hydroperiod) is another potential feedback on patch expansion. Our observations of water depth
386 control on ridge density comport with numerous studies (Givnish et al., 2008; Zwieg and Kitchens, 2008; Todd et al.,
387 2012) suggesting ridges are significantly impacted by water depths. Moreover, pattern geometry strongly influences
388 landscape hydrology (Kaplan et al. 2012, Acharya et al. 2015). As ridges expand into adjacent sloughs, they displace
389 water and alter landscape flow capacity, causing regional water levels to increase (Kaplan et al., 2012), and creating a
390 negative feedback that likely limits further ridge expansion (Cohen et al. 2011). Indeed, the RASCAL model of ridge-
391 slough development (Larsen and Harvey 2011) represents this feedback, though in that model, velocity-field feedbacks
392 alone could not impose elongation and regular patterning; disentangling sediment transport and water-level feedbacks in
393 that model, and interrogating pattern output, may enable tests of the relative importance of overlapping feedbacks at
394 different scales. We note here that because water depths equilibrate quickly, local patch expansion effects on water level
395 are distributed rapidly and evenly across the landscape. This expansion is consistent with the global limitation necessary
396 to create observed aperiodic and scale-free pattern. Therefore, water depth effects are strong candidates for the requisite
397 global feedback to induce ridge-slough formation.

398 Our results also indicate that elongated landscape features do not necessarily require pattern periodicity,
399 suggesting that spatial structures in numerous ecosystems may have been misclassified as regularly patterned, and that
400 aperiodic banding may be more prevalent than the literature suggests. Invoking robust criticality and directional
401 facilitation, as in Acharya et al. (2015), may be of general value for explaining aperiodic banding in other settings.

402 The ridge-slough landscape pattern has emerged as a key measure of restoration performance in one of the largest
403 and most ambitious ecosystem management endeavors ever. Enumeration of spatial pattern statistical features is a

404 prerequisite for assessing landscape condition and for comparing models with alternative landscape genesis mechanisms.
405 Our results inform the metrics for comparison between real and simulated landscape patterns, and provide insights into
406 the controls on pattern variation across the contemporary system. Given the potentially significant differences in water
407 management implied by comparative genesis explanations, these metrics of real and simulated landscapes are important
408 for restoration planning and assessment.
409

410 **References**

- 411 Acharya, S., Kaplan, D.A., Casey, S., Cohen, M.J., and Jawitz, J.W.: Coupled local facilitation and global hydrologic
412 inhibition drive landscape geometry in a patterned peatland, *Hydrology and Earth System Sciences*, 19(5), 2133-
413 2144, 2015.
- 414 Bak, P., Tang, C., and Wiesenfeld, K.: Self-organized criticality, *Phys. Rev. A*, 38, 364–374, 1989.
- 415 Borgogno, F., D’Odorico, P., Laio, F., and Ridolfi, L.: Mathematical models of vegetation pattern formation in
416 ecohydrology, *Rev. Geophys.*, 47, RG1005, 2009.
- 417 Brewer, J. S.: Site differences in the clone structure of an emergent sedge, *Cladium jamaicense*, *Aquat. Bot.*, 55, 79–91,
418 1996.
- 419 Cheng, Y., Stieglitz, M., Turk, G., and Engel, V.: Effects of anisotropy on pattern formation in wetland ecosystems,
420 *Geophys. Res. Lett.*, 38, 2011.
- 421 Clauset, A., Shalizi, C. R., and Newman, M. E.: Power-law distributions in empirical data, *SIAM Rev.*, 51, 661–703,
422 2009.
- 423 Cohen, M. J., Osborne, T. Z., Lamsal, S. J., and Clark, M. W.: Regional Distribution of Soil Nutrients-Hierarchical Soil
424 Nutrient Mapping for Improved Ecosystem Change Detection, South Florida Water Management District, West
425 Palm Beach, Florida, USA, 91 pp., 2009.
- 426 Cohen, M.J., Watts, D.L., Heffernan, J.B., and Osborne T.Z.: Reciprocal biotic control on hydrology, nutrient gradients
427 and landform in the Greater Everglades, *Crit. Rev. Environ. Sci. Technol.*, 41, 395-429, 2011.
- 428 Couteron, P.: Quantifying change in patterned semi-arid vegetation by Fourier analysis of digitized aerial photographs,
429 *Int. J. Remote Sens.*, 23, 3407–3425, 2002.
- 430 Eppinga, M. B., Rietkerk, M., Borren, W., Lapshina, E., Bleuten, W., and Wassen, M.: Regular surface patterning of
431 peatlands: confronting theory with field data, *Ecosystems*, 11, 520–536, 2008.
- 432 Eppinga, M. B., Rietkerk, M., Belyea, L., Nilsson, M., Ruiten, P., and Wassen, M.: Resource contrast in patterned
433 peatlands increases along a climatic gradient, *Ecology*, 91 (8), 2344-2355, 2010.
- 434 Foti, R., del Jesus, M., Rinaldo, A., and Rodriguez-Iturbe, I.: Hydroperiod regime controls the organization of plant
435 species in wetlands, *P. Natl. Acad. Sci. USA*, 109, 19596–19600, 2012.
- 436 Givnish, T. J., Volin, J. C., Owen, V. D., Volin, V. C., Muss, J. D., and Glaser, P. H.: Vegetation differentiation in the
437 patterned landscape of the central Everglades: importance of local and landscape drivers, *Global Ecol. Biogeogr.*,
438 17, 384–402, 2008.
- 439 Heffernan, J. B., Watts, D. L., and Cohen, M. J.: Discharge competence and pattern formation in peatlands: a meta-
440 ecosystem model of the everglades ridge-slough landscape, *PloS one*, 8, e64174, 2013.
- 441 Kaplan, D. A., Paudel, R., Cohen, M. J., and Jawitz, J. W.: Orientation matters: patch anisotropy controls discharge
442 competence and hydroperiod in a patterned peatland, *Geophys. Res. Lett.*, 39, L17401, 2012.
- 443 Kéfi, S., Rietkerk, M., Alados, C. L., Pueyo, Y., Papanastasis, V. P., ElAich, A., and De Ruiten, P. C.: Spatial vegetation
444 patterns and imminent desertification in Mediterranean arid ecosystems, *Nature*, 449, 213–217, 2007.
- 445 Kéfi, S., Rietkerk, M., Roy, M., Franc, A., De Ruiten, P. C., and Pascual, M.: Robust scaling in ecosystems and the
446 meltdown of patch size distributions before extinction, *Ecol. Lett.*, 14, 29–35, 2011.
- 447 Kéfi, S., Guttal, V., Brock, W. A., Carpenter, S. R., Ellison, A. M., Livina, V. N., Seekell, D. A., Scheffer, M., van Nes,
448 E. H., and Dakos, V.: Early warning signals of ecological transitions: methods for spatial patterns, *PloS one*, 9,
449 e92097, 2014.
- 450 Lago, M. E., Miralles-Wilhelm, F., Mahmoudi, M., and Engel, V.: Numerical modeling of the effects of water flow,
451 sediment transport and vegetation growth on the spatiotemporal patterning of the ridge and slough landscape of
452 the Everglades wetland, *Adv. Water Resour.*, 33, 1268–1278, 2010.
- 453 Larsen, L.G., Harvey, J.W., and Maglio, M.M: Mechanisms of nutrient retention and its relation to flow connectivity in

454 river–floodplain corridors, *Freshwater Science* 34, 187-205, 2015.

455 Larsen, L. G. and Harvey, J. W.: How vegetation and sediment transport feedbacks drive landscape change in the
456 Everglades and wetlands worldwide, *Am. Nat.*, 176, E66–E79, 2010.

457 Larsen, L. G. and Harvey, J. W.: Modeling of hydroecological feedbacks predicts distinct classes of landscape pattern,
458 process, and restoration potential in shallow aquatic ecosystems, *Geomorphology*, 126.3, 279-296, 2011.

459 Larsen, L. G., Harvey, J. W., and Crimaldi, J. P.: A delicate balance: ecohydrological feedbacks governing landscape
460 morphology in a lotic peatland, *Ecol. Monogr.*, 77, 591–614, 2007.

461 Larsen, L. G., Aumen, N., Bernhardt, C., Engel, V., Givnish, T., Hagerthey, S., Harvey, J., Leonard, L., McCormick, P.,
462 McVoy, C., Noe, G., Nungesser, M., Rutchey, K., Sklar, F., Troxler, T., Volin, J., and Willard, D.: Recent and
463 historic drivers of landscape change in the Everglades ridge, slough, and tree island mosaic, *Crit. Rev. Env. Sci.*
464 *Tec.*, 41, 344–381, 2011.

465 Li, H. and Wu, J.: Use and misuse of landscape indices, *Landscape Ecol.*, 19, 389–399, 2004.

466 Light, S. S. and Dineen, J. W.: *Water Control in the Everglades: a Historical Perspective*, Everglades: the Ecosystem and
467 its Restoration, St. Lucie Press, Delray Beach, Florida, 47–84, 1994.

468 Limpert, E., Stahel, W. A., and Abbt, M.: Log-normal distributions across the sciences: keys and clues, *Bioscience*, 51,
469 341–352, 2001.

470 Ludwig, J. A., Tongway, D. J., and Marsden, S. G.: Stripes, strands, or stipples: modelling the influence of three
471 landscape banding patterns on resource capture and productivity in semi-arid woodlands, Australia, *Catena*, 37,
472 257–273, 1999.

473 Mandelbrot, B. B.: *The Fractal Geometry of Nature*, Freeman, New York, 1983.

474 Manor, A. and Shnerb, N. M.: Facilitation, competition, and vegetation patchiness: from scale free distribution to
475 patterns, *J. Theor. Biol.*, 253, 838–842, 2008a.

476 Manor, A. and Shnerb, N. M.: Origin of Pareto-like spatial distributions in ecosystems, *Phys. Rev. Lett.*, 101, 268104,
477 2008b.

478 McVoy, C., Park Said, W., Obeysekera, J., VanArman, J., and Dreschel, T.: *Landscapes and Hydrology of the*
479 *Predrainage Everglades*, University Press of Florida, Gainesville, FL, 2011.

480 Mugglestone, M. A. and Renshaw, E.: Detection of geological lineations on aerial photographs using two-dimensional
481 spectral analysis, *Comput. Geosci.*, 24, 771–784, 1998.

482 Newman, M. E.: Power laws, Pareto distributions and Zipf’s law, *Contemp. Phys.*, 46, 323–351, 2005.

483 Noe, G. B., Childers, D. L., and Jones, R. D.: Phosphorus biogeochemistry and the impact of phosphorus enrichment:
484 why is the Everglades so unique?, *Ecosystems*, 4, 603–624, 2001.

485 Nungesser, M. K.: Reading the landscape: temporal and spatial changes in a patterned peatland, *Wetl. Ecol. Manag.*, 19,
486 475–493, 2011.

487 Pascual, M. and Guichard, F.: Criticality and disturbance in spatial ecological systems, *Trends Ecol. Evol.*, 20, 88–95,
488 2005.

489 Pascual, M., Roy, M., Guichard, F., and Flierl, G.: Cluster size distributions: signatures of self–organization in spatial
490 ecologies, *Philos. T. R. Soc. B*, 357, 657–666, 2002.

491 Pickett, S. T. and Cadenasso, M. L.: Landscape ecology: spatial heterogeneity in ecological systems, *Science*, 269, 331–
492 334, 1995.

493 Pisarenko, V. F. and Sornette, D.: Characterization of the frequency of extreme earthquake events by the generalized
494 Pareto distribution, *Pure Appl. Geophys.*, 160, 2343–2364, 2003.

495 RECOVER: 2014 System Status Report, Restoration Coordination and Verification Program, c/o US Army Corps of
496 Engineers, Jacksonville, FL, and South Florida Water Management District, West Palm Beach, FL, 2014.

497 Remmel, T. K. and Csillag, F.: When are two landscape pattern indices significantly different?, *J. Geogr. Syst.*, 5, 331–
498 351, 2003.

499 Rietkerk, M. and Van de Koppel, J.: Regular pattern formation in real ecosystems, *Trends Ecol. Evol.*, 23, 169–175,
500 2008.

501 Ross, M. S., Mitchell-Bruker, S., Sah, J. P., Stothoff, S., Ruiz, P. L., Reed, D. L., Jayachandran, K., and Coultas, C. L.:
502 Interaction of hydrology and nutrient limitation in the Ridge and Slough landscape of the southern Everglades,
503 *Hydrobiologia*, 569, 37–59, 2006.

504 Rutchey, K., Vilchek, L., and Love, M.: Development of a vegetation map for Water Conservation Area 3, Technical
505 Publication ERA Number 421, South Florida Water Management District, West Palm Beach, FL, USA, 2005.

506 Scanlon, T. M., Caylor, K. K., Levin, S. A., & Rodriguez-Iturbe, I. (2007). Positive feedbacks promote power-law
507 clustering of Kalahari vegetation. *Nature*, 449(7159), 209-212.

508 Science Coordination Team: The Role of Flow in the Everglades Ridge and Slough Landscape, South Florida Ecosystem
509 Restoration Working Group, West Palm Beach, FL, 2003.

510 Stauffer, D. and Aharony, A.: Introduction to percolation theory, Taylor and Francis, London, 1991.

511 Sullivan, P. L., Price, R. M., Miralles-Wilhelm, F., Ross, M. S., Scinto, L. J., Dreschel, T. W., Sklar, F. H., and Cline, E.:
512 The role of recharge and evapotranspiration as hydraulic drivers of ion concentrations in shallow groundwater on
513 Everglades tree islands, Florida (USA), *Hydrol. Process.*, 28, 293–304, 2014.

514 Todd, M. J., Muneeppeerakul, R., Pumo, D., Azaele, S., Miralles-Wilhelm, F., Rinaldo, A., and Rodriguez-Iturbe, I.:
515 Hydrological drivers of wetland vegetation community distribution within Everglades National Park, Florida,
516 *Adv. Water Resour.*, 33, 1279–1289, 2010.

517 Turner, M. G.: *Landscape Ecology in Theory and Practice: Pattern and Process*, Springer-Verlag, New York, 2001.

518 Turner, M. G.: Landscape ecology: what is the state of the science?, *Annu. Rev. Ecol. Evol. S.*, 36, 319–344, 2005.

519 von Hardenberg, J., Kletter, A. Y., Yizhaq, H., Nathan, J., and Meron, E.: Periodic vs. scale-free patterns in dryland
520 vegetation, *P. R. Soc. B*, 277, 1771–1776, 2010.

521 Watts, D. L., Cohen, M. J., Heffernan, J. B., and Osborne, T. Z.: Hydrologic modification and the loss of self-organized
522 patterning in the ridge–slough mosaic of the Everglades, *Ecosystems*, 13, 813–827, 2010.

523 Weerman, E. J., Van Belzen, J., Rietkerk, M., Temmerman, S., Kéfi, S., Herman, P. M. J., and de Koppel, J. V.: Changes
524 in diatom patch-size distribution and degradation in a spatially self-organized intertidal mudflat ecosystem,
525 *Ecology*, 93, 608–618, 2012.

526 Wetzel, P. R., van der Valk, A. G., Newman, S., Gawlik, D. E., Troxler Gann, T., Coronado-Molina, C. A., Childers, D.
527 L., and Sklar, F. H.: Maintaining tree islands in the Florida Everglades: nutrient redistribution is the key, *Front.*
528 *Ecol. Environ.*, 3, 370–376, 2005.

529 Wetzel, P. R., van der Valk, A. G., Newman, S., Coronado, C. A., Troxler-Gann, T. G., Childers, D. L., Orem, W. H., and
530 Sklar, F. H.: Heterogeneity of phosphorus distribution in a patterned landscape, the Florida Everglades, *Plant*
531 *Ecol.*, 200, 83–90, 2009.

532 Wu, Y., Wang, N., Rutchey, K.: An analysis of spatial complexity of ridge and slough patterns in the Everglades
533 ecosystem, *Ecol. Complex.*, 3, 183–192, 2006.

534 Yuan, J., Cohen, M. J., Kaplan, D. A., Acharya, S., Larsen, L. G., and Nungesser, M. K.: Linking metrics of landscape
535 pattern to hydrological process in a lotic wetland, *Landscape Ecol.*, in review, 2015.

536 Zweig, C. L. and Kitchens, W. M.: Effects of landscape gradients on wetland vegetation communities: information for
537 large-scale restoration, *Wetlands*, 28, 2008.

538
539
540

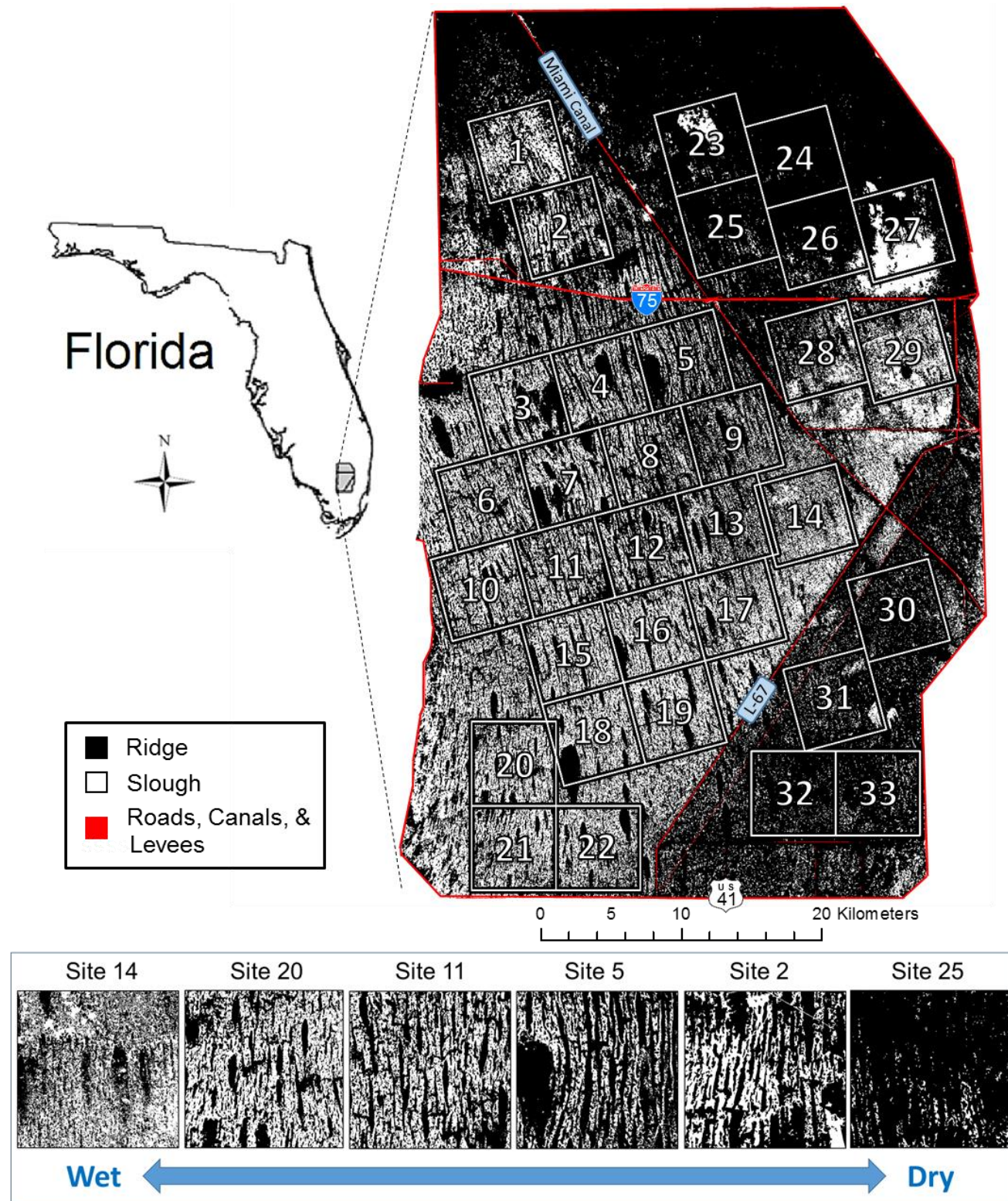
541

542 **Figure Legends**

543 Figure 1: Study area and site locations, including major roads, canals, and levees for the primary map (M1). Sites
544 spanning the pattern gradient in WCA3 are shown in the bottom panel. Two additional maps (supplementary
545 information) were used to corroborate the primary results.

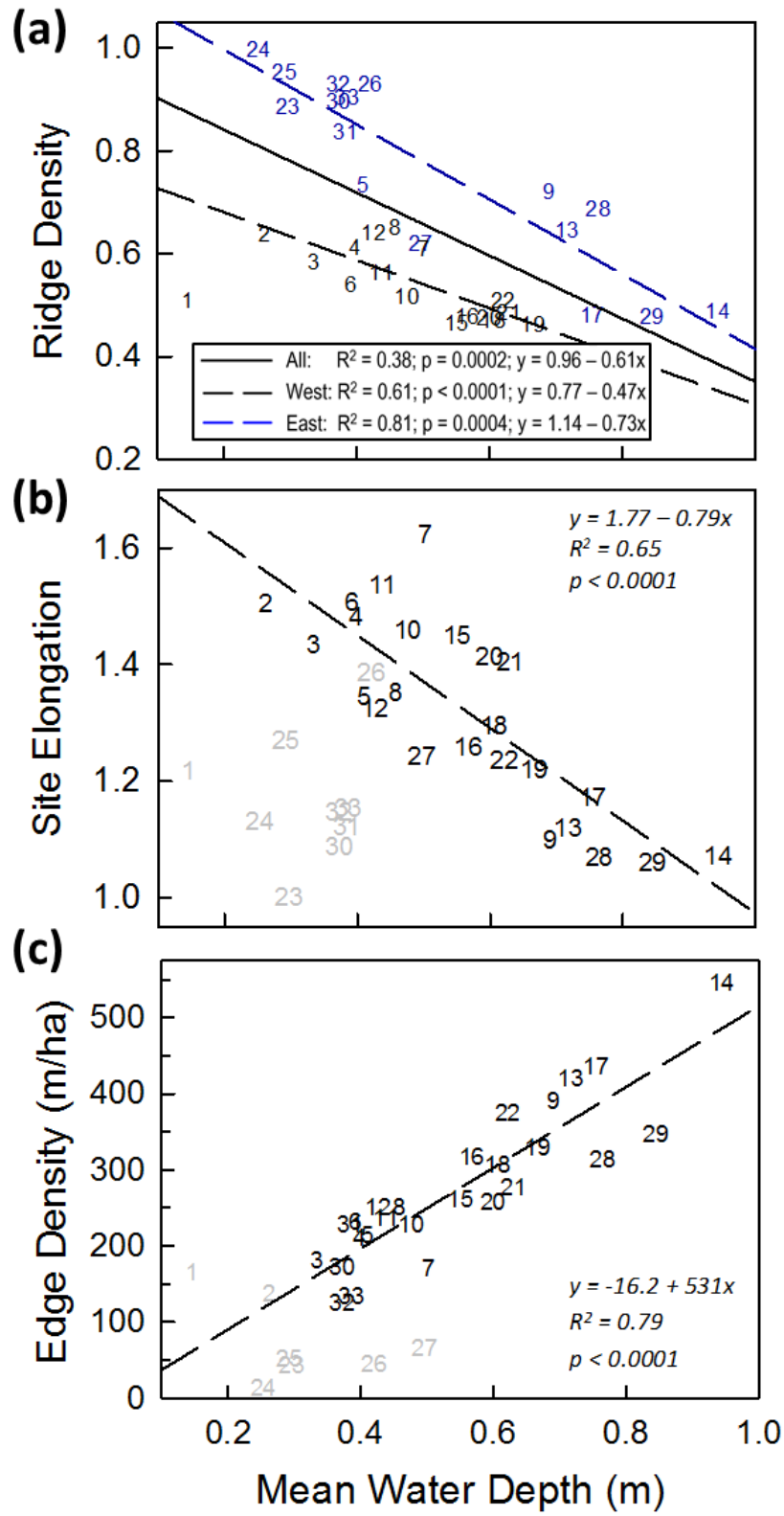
546 Figure 2: **(a)** Ridge density is negatively correlated with mean water depth. Eastern sites (blue) show consistently higher
547 ridge densities than those in the west (black). Trends associated with east–west segregation (dashed lines) show
548 much stronger relationships than the composite trend (solid line). Site 1 was omitted due to possible
549 misclassification. **(b)** Site elongation shows a strong negative relationship with mean water depth. Sites with ridge
550 densities greater than 0.8 (indicated in grey) were omitted from regressions and show elongation values lower than
551 expected from this trend. **(c)** Edge density is positively correlated to mean water depth indicating higher
552 perimeters in deeper sites. Sites indicated in grey were mapped at lower resolution, and were omitted from
553 regressions. The relationships observed for site elongation and edge density are both consistent with patches
554 becoming disaggregated with increased water depth.

555 Figure 3: **(a)** Lateral r spectra (limited to $\pm 10^\circ$ perpendicular to the pattern) monotonically decreased with no evidence of
556 peaks, indicating aperiodic behavior in the direction of presumed regularity. **(b)** Longitudinal r spectra (limited to
557 $\pm 10^\circ$ in the direction parallel to the pattern) shows similar monotonic behavior. The form for both lateral and
558 longitudinal directions is similar, with both exhibiting a mixture of power-law and exponential behavior. The
559 location of the exponential-like curvature appears to be influenced by both orientation and pattern condition,
560 suggesting a weak-acting scale-dependent mechanism. **(c)** Patch size distributions across sites are well described
561 by the generalized Pareto distribution (red lines). Sites with high ridge densities (e.g. sites 2, 5 and 25) have
562 maximum patch sizes much greater than expected from the GP distribution. Conversely, sites in excessively
563 inundated sections (e.g. site 20) show slightly steeper tails, consistent with a lognormal distribution (blue lines),
564 though not enough to rule out the GP.



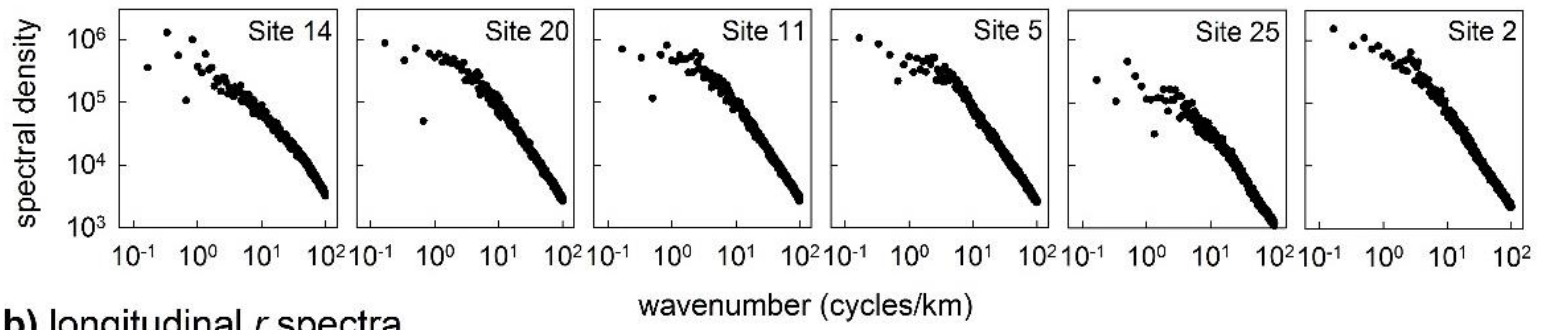
565
566
567

Figure 1

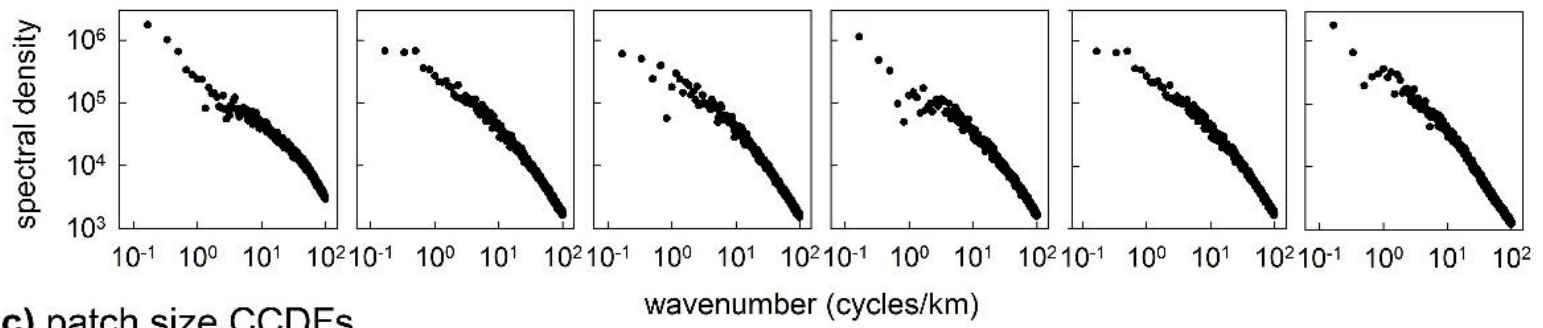


569 Figure 2

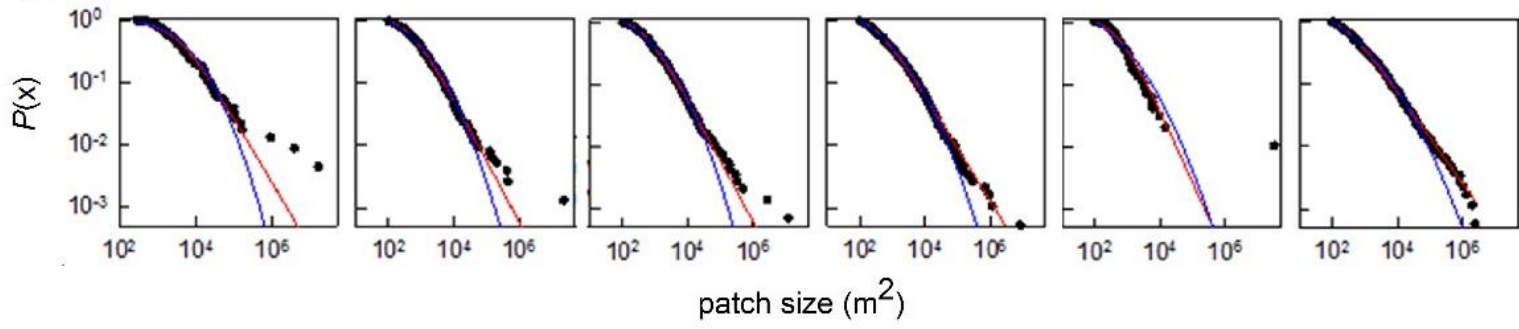
a) lateral r spectra



b) longitudinal r spectra



c) patch size CCDFs



570
571

Figure 3